Multiphoton ionization of He by using intense high-order harmonics in the soft-x-ray region

Hirokazu Hasegawa,[1,*] Eiji J. Takahashi,[1,†] Yasuo Nabekawa,[1] Kenichi L. Ishikawa,[2] and Katsumi Midorikawa[1,‡]
[1]*Laser Technology Laboratory, RIKEN, 2-1 Hirosawa, Wako, Saitama 351-0198, Japan*
[2]*Department of Quantum Engineering and Systems Science, Graduate School of Engineering, University of Tokyo, 7-3-1 Hongo, Bunkyo-ku, Tokyo, 113-8656, Japan*
(Received 13 September 2004; published 14 February 2005)

We report on the multiphoton ionization processes in the soft-x-ray region ($\lambda \leqslant 30$ nm). On the basis of the measured time-of-flight spectra for both ions and electrons obtained using intense soft-x-ray pulses produced by high-order harmonics, the cross sections of the two-photon double ionization and above-threshold ionization of He are estimated. The high-intensity soft-x-ray radiation achieved by phase-matched high-order harmonics enables the investigation of these nonlinear optical processes, which were beyond the reach of conventional light sources.

DOI: 10.1103/PhysRevA.71.023407 PACS number(s): 32.80.Rm, 42.65.Ky

The study of double-ionization processes following the absorption of photons is of paramount importance in physics as it gives insights into strongly correlated quantum dynamics. The observation of the energies and angular distributions of the ions and/or electrons produced by double ionization provides important information concerning the electron correlation. Helium is the most important and simplest system for research concerning such electron correlation.

In the short-wavelength, low-intensity region, experimental and theoretical works on the single-photon double ionization of He have been progressing considerably well using synchrotron radiation (reviewed by Briggs and Schmidt [1]). Also, nonsequential double ionization of He using long-wavelength ($\sim$800 nm), high-intensity laser pulses has been investigated extensively [2–6]. Between these two extremes, there is another important area of double ionization. This is two-photon double ionization (TPDI) of He by intense soft-x-ray radiation. This ionization process cannot be induced until the photon energy exceeds half the ionization energy of TPDI, i.e., $h\nu \geqslant 39.5$ eV. Anticipating the development of intense coherent soft-x-ray sources, many theoretical studies of the two-photon ionization processes of He including TPDI have been reported [7–16].

The observation of two-photon ionization processes in the soft-x-ray region has also been a very attractive and challenging area of research in quantum electronics since the first observation of second-harmonic generation and two-photon excitation in the visible range in 1961. No observation of nonlinear optical process by soft-x-ray photons, however, has been reported because of a lack of intense short-wavelength light sources although some researchers have observed nonlinear processes in vacuum ultraviolet region [17–20]. Recently, nonlinear two-photon processes (above-threshold ionization) of rare gas atoms (He, Ar, Xe) by using the fifth harmonic (25 eV) of a KrF laser are reported [21]. However, this photon energy of 25 eV cannot induce TPDI of He. This situation has changed recently due to the advent of an intense coherent soft-x-ray source based on high-order harmonics (HH). We have produced the highest peak photon flux ($\sim 10^{26}$ photons/mm^2 mrad^2 s) in the soft-x-ray region (the 27th harmonic of Ti:sapphire laser; a wavelength of 29.6 nm and a photon energy of 41.8 eV) by high-order harmonics [22]. When such a harmonic pulse was focused with an off-axis parabolic multilayer mirror, the focused intensity attained 1×10^{14} W/cm^2 [23], which is considered to be sufficient for inducing nonlinear optical phenomena in the soft-x-ray region.

In this paper, we report on the observation of multiphoton ionization processes using 41.8 eV soft-x-ray photons and the estimation of the cross sections of TPDI and above-threshold ionization of He. Intense soft x-ray generated by phase-matched HH enables the investigation of these nonlinear optical processes.

The relevant energy diagram of He, He^+, and He^{2+} and ionization pathways using 41.8 eV photons is shown in Fig. 1 when two-photon absorption occurs. The possible ionization pathways are as follows:

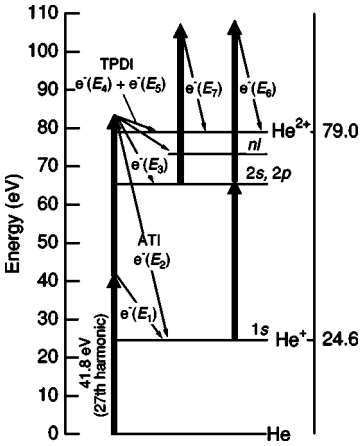

FIG. 1. Relevant energy diagram of He, He^+, and He^{2+} and ionization pathways of 41.8 eV photon.

*Electronic address: hase@riken.jp
†Present address: Department of Vacuum UV photoscience, Institute for Molecular Science.
‡Electronic address: kmidori@riken.jp

$$\mathrm{He} + h\nu \rightarrow \mathrm{He}^+(1s) + e^-(E_1)\ [\text{one-photon single ionization}(\sigma^+)], \tag{1}$$

$$\mathrm{He} + 2h\nu \rightarrow \mathrm{He}^+(1s) + e^-(E_2)\ [\mathrm{ATI}(\sigma_{\mathrm{ATI}})], \tag{2}$$

$$\mathrm{He} + 2h\nu \rightarrow \mathrm{He}^+(nl) + e^-(E_3)\ [\text{ionization with excitation}(\sigma^+_{nl})], \tag{3}$$

$$\mathrm{He} + 2h\nu \rightarrow \mathrm{He}^{2+} + e^-(E_4) + e^-(E_5)\ [\mathrm{TPDI}(\sigma_{\mathrm{TPDI}})], \tag{4}$$

$$\mathrm{He} + h\nu \xrightarrow{\sigma^+} \mathrm{He}^+(1s) + e^-(E_1), \tag{5}$$

$$\mathrm{He}^+(1s) + 2h\nu \xrightarrow{\sigma^{2+}} \mathrm{He}^{2+} + e^-(E_6)\ [\text{sequential double ionization } 1(\sigma_{\mathrm{seq1}})],$$

$$\mathrm{He} + 2h\nu \xrightarrow{\sigma^+_{nl}} \mathrm{He}^+(nl) + e^-(E_3), \tag{6}$$

$$\mathrm{He}^+(nl) + h\nu \xrightarrow{\sigma^{2+}_{nl}} \mathrm{He}^{2+} + e^-(E_7)\ [\text{sequential double ionization } 2(\sigma_{\mathrm{seq2}})].$$

Here, $\mathrm{He}^+(1s)$ and $\mathrm{He}^+(nl)$ represent the ground state and excited states (principle quantum number $n \geqslant 2$ and angular momentum l) of He^+, respectively. The photoelectron energies of each pathway are $E_1 = 17.2$ eV, $E_2 = 59.0$ eV, and $E_3 = 18.2$ eV for $n=2$, $E_4 + E_5 = 4.6$ eV, $E_6 = 29.2$ eV, and $E_7 = 12.6$ eV for $n=2$ at a photon energy $h\nu$ of 41.8 eV.

All the ionization pathways except for (1) include two-photon (nonlinear) processes. Pathway (4) (TPDI) is the most distinct feature of the ionization process induced by absorption of high-intensity soft-x-ray photons. In addition to being a nonlinear process, this pathway produces a correlated electron pair. This electron pair shares the excess energy ($\Delta E = 2h\nu - IP_{\mathrm{He}^{2+}} = E_4 + E_5 = 4.6$ eV). This ionization process does not occur by using a photon energy lower than $IP_{\mathrm{He}^{2+}}/2 = 39.5$ eV, corresponding to a wavelength longer than 31.4 nm (that of the 25th harmonic of the Ti:sapphire laser). Pathway (2), known as an above-threshold ionization (ATI) process [24], is also significant because it competes with TPDI. It is important in atomic physics to determine how many electrons go into each pathway.

Concerning the production of the doubly charged He^{2+}, the nonlinear process is required through pathways (4)–(6). Therefore, the observation of He^{2+} provides clear evidence for the nonlinear interaction in soft-x-ray spectral region. The ATI process also occurs by two-photon absorption. Therefore, the observation of ATI electrons provide such evidence as well as significant information concerning the competition of the ATI and TPDI processes. However, since the final charge state of this process is single-ionized ion, it is impossible to detect it separately from the single-ionized ions produced by single-photon absorption. Therefore, we observe photoelectron energy spectra for detection of the ATI process instead of ion measurement. Although TPDI process also produces characteristic electrons, TPDI signal of produced electron is difficult to be detected due to low-energy electrons produced with residual weak harmonics as described below.

TABLE I. Ionization cross sections, in units of 10^{-52} cm^4 s, of the theoretical calculations and this experimental work.

Researchers	ATI	Excited states[a]	TPDI
Nikolopoulos *et al.* (Ref. [8])[b]		(0.48)	0.019
Mercouris *et al.* (Ref. [10])[c]			0.015
Nakajima *et al.* (Ref. [12])[d]	1.0	61[e]	8.1
Colgan *et al.* (Ref. [13])[d]	1.0	14	1.2
Laulan *et al.* (Ref. [14])[d]		(15.7)	1.7
Feng *et al.* (Ref. [15])[c]		(200)	0.25
Ishikawa (Ref. [16])[c]	0.53	56[e]	0.30
This work[c]	2	100[f]	0.4

[a]The values in parentheses are the sum of ATI and excited states.
[b]42.5 eV.
[c]41.8 eV.
[d]45 eV.
[e]Only the 2*s*, 2*p* excited states.
[f]Only the 2*p* excited state.

Theoretical calculations of the cross section of each ionization pathway have been reported by many groups [7–16]. These results are summarized in Table I. The reported cross sections of ATI and TPDI show a difference larger than one order of magnitude. Thus, the measurement of ATI and TPDI provides very valuable data for theoretical calculation and advances the understanding of electron correlation.

In the experiment, we measured the mass spectra of ions with a conventional time-of-flight (TOF) mass spectrometer with $L_{\mathrm{TOF}} = 33$ cm drift length and a microchannel plate (MCP) detector of $d = 2.54$ cm diameter. Three electrodes in the TOF spectrometer apply extraction and acceleration voltages for ion experiment and ground voltages for photoelectron experiment. Several harmonics around the 27th harmonic generated with a femtosecond pulse of a Ti:sapphire laser (a pulse width τ of 23 fs, a central wavelength of 800 nm, a pulse energy of 20 mJ/pulse, and a repetition rate of 10 Hz) were separated from the intense fundamental pulse with beam splitter(s) of silicon or silicon carbide [25], then sent to a spherical mirror multilayered coat of silicon carbide/magnesium (SiC/Mg) with a radius of curvature of 100 mm in the interaction chamber. The SiC/Mg mirror has the reflectivity of 24% at the 27th harmonic. The polarization of laser and harmonics is parallel to the TOF axis. The energy of the 27th harmonic was estimated to be 24 nJ/pulse in the interaction region with 50% energy fluctuation. The spot size was estimated to be $\omega_0 = 3.1$ μm from a separate experiment [26]. Thus, the intensity of the 27th harmonic was estimated to be $I = 7 \times 10^{12}$ W/cm^2. Here, we regard the pulse width of the 27th harmonic to be the same as that of the fundamental. Since the pulse width of the harmonics is shorter than that of the fundamental [18], our estimation of

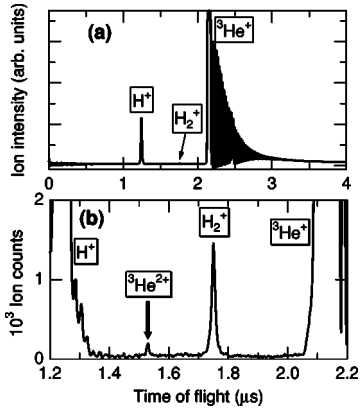

FIG. 2. TOF mass spectra of ^{3}He.

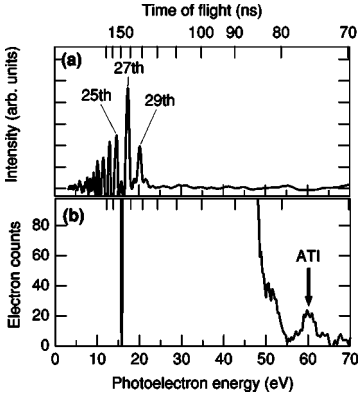

FIG. 3. Photoelectron spectra of He. (a) A wide spectrum averaged using an oscilloscope. (b) An expanded view of the photoelectron spectrum measured by electron counting. The bottom axis represents photoelectron energy. The top axis corresponds to the TOF of electrons.

the harmonic intensity may give lower limit. The confocal parameter was also determined to be 250 μm from the same experiment [26]. Based on the values of the confocal parameter and spot size, the interaction volume V is estimated to be 3.5×10^{-9} cm^3.

The TOF spectra were recorded on a oscilloscope and/or a computer, then averaged to assign the strong peaks which originated from the single-photon process and also processed for counting the signals which exceed the threshold voltage to find the weak signals in the spectra. The isotope ^{3}He was used as the sample gas in the ion experiment to avoid the overlap of signals between $^4He^{2+}$ and H_2^+, the latter of which originated from residual water in the vacuum chamber. The sample gas is introduced continuously into the interaction chamber through the variable leak valve up to 1×10^{-4} Torr. Therefore, the target gas density at the interaction region is determined to be $d=3.2\times10^{12}$ cm^{-3}. The number of shots accumulated (N_{shot}) is 10 000.

Figure 2 shows a spectrum of the ions produced by the interaction between the focused harmonic pulses and ^{3}He. The strongest peak of 2.15 μs can be assigned to $^3He^+$. The production of $^3He^+$ results dominantly from the one-photon absorption of ^{3}He. The effects of the consumption of neutral He is negligible under our experimental conditions.

The peak at 1.53 μs of the TOF spectrum, shown in Fig. 2, can be assigned as doubly charged $^3He^{2+}$. The peaks at the TOF of 1.24 μs and 1.75 μs correspond to the signals of H^+ and H_2^+ ions originating from residual H_2O molecules in the vacuum chamber, respectively. The signal of $^3He^{2+}$ clearly appears between the H^+ signal and H_2^+ signal. The generation of doubly charged He^{2+} confirms the first observation of a nonlinear optical process (two-photon absorption) in the soft-x-ray region.

We carried out a subsequent experiment to measure the photoelectron spectra (PES) so that we could estimate the contribution of TPDI to the ionization process responsible for the production of He^{2+}. Unfortunately, a few harmonics other than the 27th were partially reflected by the SiC/Mg mirror, thus disturbing the photoelectron spectra in the energy range of 0–4.6 eV, in which TPDI electrons are expected to appear, due to the large signals of the single-photon ionization processes. Accordingly, while we could not observe electrons from the TPDI process, we succeeded in detecting the ATI electrons. The averaged spectrum of the TOF experiment for electrons is shown in Fig. 3(a). The setup and signal processing used in this experiment are similar to those used in the ion TOF experiment except for the use of the TOF chamber for the electrons. The sample gas is introduced into the interaction chamber through the pulsed valve synchronized with harmonic pulses because electron signal is very weak. The strongest peak at 142 ns corresponds to the photoelectron which accompanies the single-photon ionization from He to $He^+(1s)$ of the 27th harmonic. The other photoelectron signals, which are originated from single-photon ionization, appear at 158 ns for the 25th harmonic and 131 ns for the 29th harmonic. With the counting measurement ($N_{\mathrm{shot}}=30\,000$) of the spectrum, we found the remarkable feature of photoelectron at the TOF of 76 ns as shown in Fig. 3(b) by an arrow. By converting the TOF to kinetic energy using the assigned peaks, this fast (high-energy) peak was ascribed to photoelectrons with an energy of 59 eV produced via the ATI of the 27th harmonic. This result is more evidence of the nonlinear optical process. The electron signal gives us the nonlinear cross section for ATI, σ_{ATI}, which should be compared with σ_{TPDI} to investigate the competition of the two nonsequential ionization processes.

We can extract the quantitative information of the nonlinear processes detailed in Fig. 1 from the experiments of the ions and the electrons. In our theoretical model, harmonic intensity keeps constant value ($I=7\times10^{12}$ W/cm^2) over the focal volume. Although the TPDI signal of the electrons could not be determined directly, we can estimate the cross section of this ionization process, σ_{TPDI}, using the number of detected doubly charged ions ($N_{\mathrm{ion}}{}^{2+}=200$) as follows.

Ionization pathways (4)–(6) contribute to the production of observed He^{2+}. So, we define the combined (total) cross section for the generation of He^{2+} ($\sigma_{\mathrm{ion}}{}^{2+}$) as

$$\sigma_{\mathrm{ion}}{}^{2+}=\sigma_{\mathrm{TPDI}}+\sigma_{\mathrm{seq1}}+\sigma_{\mathrm{seq2}}$$
$$=\sigma_{\mathrm{TPDI}}\left(1+\frac{\sigma_{\mathrm{seq2}}}{\sigma_{\mathrm{TPDI}}}\right)+\sigma_{\mathrm{seq1}}, \qquad (7)$$

where $\sigma_{\mathrm{seq1}}=\sigma^+(I/h\nu)\tau\sigma^{2+}$ and σ_{seq2}

$=\Sigma_{nl}^{\text{all excited states}}[\sigma_{nl}^{2+}(I/h\nu)\tau]\sigma_{nl}^{+}$ are the effective cross sections of sequential double ionizations 1 and 2, respectively. σ^{+} and σ^{2+} are the cross sections of the He to $He^{+}(1s)$ and of the $He^{+}(1s)$ to He^{2+} ionization processes, respectively. ${\sigma_{nl}}^{+}$ and ${\sigma_{nl}}^{2+}$ are the ionization cross sections of the He to $He^{+}(nl)$ ionization process with two-photon absorption and of the $He^{+}(nl)$ to He^{2+} ionization process with single-photon absorption, respectively. The number of detected He^{2+} ions is represented by ${N_{\text{ion}}}^{2+}={\sigma_{\text{ion}}}^{2+}(I/h\nu)^2\tau N_{\text{He}}N_{\text{shot}}\epsilon_{\text{ion}}$, where N_{He} is the number of He atoms in the interaction region, which is estimated to be 1.2×10^{4} from the measurement of the pressure, and ϵ_{ion} of 0.6 is the ion detection efficiency of the ion detector [28]. The combined cross section ${\sigma_{\text{ion}}}^{2+}$ is calculated to be 1×10^{-52} cm^4 s from this relation and ${N_{\text{ion}}}^{2+}$ is derived from the experiment. Thus, we found the left-hand side of Eq. (7). The second term on the right-hand side of Eq. (7), σ_{seq1} is obtained from $\sigma^{2+}=2.9\times10^{-52}$ cm^2, which can be exactly determined by quantum calculation since He^{+} is a hydrogenlike system [11,27], and $\sigma^{+}=2.86\times10^{-18}$ cm^2, which is taken from the experiment [29], resulting in a σ_{seq1} of 2×10^{-53} cm^4 s. Therefore, the remaining unknown value in Eq. (7) is $\sigma_{\text{seq2}}/\sigma_{\text{TPDI}}$ which is needed to estimate σ_{TPDI}.

With the assumption that the first excited state $n=2$, $l=1$ is the dominant contribution of the excited state of He^{+} to σ_{seq2}, which is theoretically supported by calculation [11,16], the ratio $\sigma_{\text{seq2}}/\sigma_{\text{TPDI}}$ can be approximated as

$$\sigma_{\text{seq2}}/\sigma_{\text{TPDI}} \sim (I/h\nu)\tau{\sigma_{2p}}^{2+}({\sigma_{2p}}^{+}/\sigma_{\text{TPDI}}). \tag{8}$$

The ratio of the cross sections ${\sigma_{2p}}^{+}/\sigma_{\text{TPDI}}$ in Eq. (8) should be ~332 making the same assumption because Feng and van der Hart and other research groups reported the theoretical value of the ratio $\Sigma_{nl}{\sigma_{nl}}^{+}/\sigma_{\text{TPDI}}$ consistently, as described in Ref. [15]. Using the result of the exact calculation, ${\sigma_{2p}}^{2+}$ is 1.2×10^{-19} cm^2. Thus, we can find the left-hand side of Eq. (8) is ~1. Finally, we conclude that σ_{TPDI} is 4×10^{-53} cm^4 s because the rest of the values in Eq. (7) have already been estimated.

The cross section of ATI, σ_{ATI}, can also be estimated from the number of observed ATI electrons, $N_{\text{ATI}}=20$ in this experiment. The number of observed ATI electrons, N_{ATI}, is described to be $N_{\text{ATI}}=\sigma_{\text{ATI}}(I/h\nu)^2\tau N_{\text{He}}N_{\text{shot}}\epsilon_{\text{elec}}$, where $\epsilon_{\text{elec}}=1.3\times10^{-3}$ is the detection efficiency of ATI electrons. This detection efficiency ϵ_{elec} is estimated from the angular distribution of the ATI electrons and MCP detection efficiency for electrons [=0.7 (Ref. [30])]. For the collection efficiency attributed to the angular distribution of ATI electron, we have to consider two different final states as follows:

$$\text{He}+2h\nu\rightarrow \text{He}^{+}(1s)+e^{-}(l=0),\quad L=0, \tag{9}$$

$$\text{He}+2h\nu\rightarrow \text{He}^{+}(1s)+e^{-}(l=2),\quad L=2, \tag{10}$$

where L is the total angular momentum. The angular distributions of each pathway, $f_L(\theta,\phi)$, are represented as follows:

$$f_0(\theta,\phi)=\frac{1}{4\pi}, \tag{11}$$

$$f_2(\theta,\phi)=\frac{5}{16\pi}(3\cos^2\theta-1)^2, \tag{12}$$

where θ and ϕ represent the polar angle and the azimuthal angle with respect to the harmonic polarization, respectively. In fact, there is the interference effect because these two pathways occur simultaneously. However, the calculation predicts that the contribution of the pathway with $L=0$ is five times smaller than that of the pathway with $L=2$ [16]. Therefore, we consider only the angular distribution with $L=2$. The collection efficiency based on the angular distribution $\epsilon_{\text{elec}}^{\text{angular}}$ is

$$\begin{aligned}\epsilon_{\text{elec}}^{\text{angular}} &= \int d\Omega f_2(\theta,\phi)\\ &= \int_0^{2\pi} d\phi \int_0^{\theta_{\text{MCP}}=2.2^\circ} d\theta f_2(\theta,\phi)\sin\theta\\ &= 1.8\times10^{-3},\end{aligned} \tag{13}$$

where $\theta_{\text{MCP}}=\tan^{-1}(d/2L_{\text{TOF}})$ is the maximum polar angle viewing MCP. As a result, we obtain the detection efficiency of electron, $\epsilon_{\text{elec}}=1.3\times10^{-3}$.

The PES signal measured at the time when harmonic pulses and gas jet are synchronized is ten times larger than that measured when those are not synchronized. In these two conditions, the static gas pressure in the interaction chamber keeps 1×10^{-4} Torr. Since the PES signal at asynchronized timing reflects the static gas pressure, the sample gas density in the interaction region at the synchronized condition is determined to be $d=3.2\times10^{13}$ cm^{-3} (1×10^{-3} Torr). Considering that the total number of He atoms in the interaction volume (N_{He}) is 1.2×10^{5}, we can determine the cross section of ATI, σ_{ATI}, to be 2×10^{-52} cm^4 s using this relation. This value agrees with the theoretically calculated values [12,13,16] (see Table I) within a factor of 4. It should be noted that their cross-section values include the experimental error. The largest error is originated from the fluctuation of the harmonic energy. If the harmonic intensity is two times larger than our estimated intensity, the cross section of TPDI becomes zero. On the other hand, if the harmonic intensity is a half of our estimated intensity, the cross section of TPDI becomes 2.9×10^{-52} cm^4 s.

In conclusion, the two-photon ionization of He with intense high-order harmonics was investigated and then nonlinear optical processes were observed in the soft- x-ray region by observation of the highest peak photon flux of the phase-matched harmonics. From the yields of He^{2+} and photoelectrons, the cross sections of TPDI and ATI were estimated. We believe that our results will lead to a new research area in nonlinear optics in the soft-x-ray region as well as correlated quantum dynamics.

This research was supported by Ministry of Education, Culture, Sports, Science, and Technology Grant-in-Aid for Scientific Research on Priority Areas under Grant No. 14077222 and Grant-in-Aid for Young Scientists (A) under Grant No. 16686006 and Grant-in-Aid for Young Scientists (B) under Grant Nos. 15760034 and 16740237 and by the Special Postdoctoral Researchers Program of the Institute of Physical and Chemical Research (RIKEN).

[1] J. S. Briggs and V. Schmidt, J. Phys. B **33**, R1 (2000).
[2] D. N. Fittinghoff, P. R. Bolton, B. Chang, and K. C. Kulander, Phys. Rev. Lett. **69**, 2642 (1992).
[3] K. Kondo, A. Sagisaka, T. Tamida, Y. Nabekawa, and S. Watanabe, Phys. Rev. A **48**, R2531 (1993).
[4] Th. Weber, M. Weckenbrock, A. Staudte, L. Spielberger, O. Jagutzki, V. Mergel, F. Afaneh, G. Urbasch, M. Vollmer, H. Giessen, and R. Dörner, Phys. Rev. Lett. **84**, 443 (2000).
[5] B. Walker, B. Sheehy, L. F. DiMauro, P. Agostini, K. J. Schafer, and K. C. Kulander, Phys. Rev. Lett. **73**, 1227 (1994).
[6] Th. Weber, M. Weckenbrock, A. Staudte, M. Hattass, L. Spielberger, O. Jagutzki, V. Mergel, H. Schmidt Böcking, G. Urbasch, H. Giessen, H. Bräuning, C. L. Cocke, M. H. Prior, and R. Dörner, Opt. Express **8**, 368 (2001).
[7] M. S. Pindzola and F. Robicheaux, J. Phys. B **31**, L823 (1998).
[8] L. A. A. Nikolopoulos and P. Lambropoulos, J. Phys. B **34**, 545 (2001).
[9] J. S. Parker, L. R. Moore, K. J. Meharg, D. Dundas, and K. T. Taylor, J. Phys. B **34**, L69 (2001).
[10] T. Mercouris, C. Haritos, and C. A. Nicolaides, J. Phys. B **34**, 3789 (2001).
[11] K. Ishikawa and K. Midorikawa, Phys. Rev. A **65**, 043405 (2002).
[12] T. Nakajima and L. A. A. Nikolopoulos, Phys. Rev. A **66**, 041402 (R) (2002).
[13] J. Colgan and M. S. Pindzola, Phys. Rev. Lett. **88**, 173002 (2002).
[14] S. Laulan and H. Bachau, Phys. Rev. A **68**, 013409 (2003).
[15] L. Feng and H. W. van der Hart, J. Phys. B **36**, L1 (2003).
[16] K. L. Ishikawa (unpublished).
[17] D. Xenakis, O. Faucher, D. Charalambidis, and C. Fotakis, J. Phys. B **29**, L457 (1996).
[18] Y. Kobayashi, T. Sekikawa, Y. Nabekawa, and S. Watanabe, Opt. Lett. **23**, 64 (1998).
[19] N. A. Papadogiannis, L. A. A. Nikolopoulos, D. Charalambidis, G. D. Tsakiris, P. Tzallas, and K. Witte, Phys. Rev. Lett. **90**, 133902 (2003).
[20] P. Tzallas, D. Charalambidis, N. A. Papadogiannis, K. Witte, and G. D. Tsakiris, Nature (London) **426**, 267 (2003).
[21] N. Miyamoto, M. Kamei, D. Yoshitomi, T. Kanai, T. Sekikawa, T. Nakajima, and S. Watanabe, Phys. Rev. Lett. **93**, 083903 (2004).
[22] E. Takahashi, Y. Nabekawa, T. Otsuka, M. Obara, and K. Midorikawa, Phys. Rev. A **66**, 021802(R) (2002).
[23] H. Mashiko, A. Suda, and K. Midorikawa, Opt. Lett. **29**, 1927 (2004).
[24] P. Agostini, F. Fabre, G. Mainfray, and G. Petite, Phys. Rev. Lett. **42**, 1127 (1979).
[25] E. J. Takahashi, H. Hasegawa, Y. Nabekawa, and K. Midorikawa, Opt. Lett. **29**, 507 (2004).
[26] E. J. Takahashi, Y. Nabekawa, H. Mashiko, H. Hasegawa, A. Suda, and K. Midorikawa, IEEE J. Select. Topics Quantum Electron (to be published).
[27] F. T. Chan and C. L. Tang, Phys. Rev. **185**, 42 (1969).
[28] J. L. Wiza, Nucl. Instrum. Methods **162**, 587 (1979).
[29] J. A. R. Samson, Z. X. He, L. Yin, and G. N. Haddad, J. Phys. B **27**, 887 (1994).
[30] M. Galanti, R. Gott, and J. F. Renaud, Rev. Sci. Instrum. **42**, 1818 (1971).